

UC San Diego

UC San Diego Previously Published Works

Title

An in vivo biosensor for neurotransmitter release and in situ receptor activity

Permalink

<https://escholarship.org/uc/item/96b4m0cv>

Journal

Nature Neuroscience, 13(1)

ISSN

1097-6256

Authors

Nguyen, Quoc-Thang
Schroeder, Lee F
Mank, Marco
[et al.](#)

Publication Date

2010

DOI

10.1038/nn.2469

Peer reviewed



Published in final edited form as:

Nat Neurosci. 2010 January ; 13(1): 127–132. doi:10.1038/nn.2469.

An *in vivo* biosensor for neurotransmitter release and *in situ* receptor activity

Quoc-Thang Nguyen^{#1}, Lee F. Schroeder^{#2,3}, Marco Mank⁴, Arnaud Muller¹, Palmer Taylor⁵, Oliver Griesbeck⁴, and David Kleinfeld^{1,3,6}

¹ Physics Department, UCSD, La Jolla, CA

² Medical Scientist Training Program, UCSD, La Jolla, CA

³ Graduate Program in Neurosciences, UCSD, La Jolla, CA

⁴ Max-Planck Institut für Neurobiologie, Martinsried, Germany

⁵ Skaggs School of Pharmacy and Pharmaceutical Sciences, UCSD, La Jolla, CA

⁶ Center for Neural Circuits and Behavior, UCSD, La Jolla, CA

These authors contributed equally to this work.

Abstract

Tools from molecular biology, in combination with *in vivo* optical imaging techniques, provide new mechanisms to noninvasively observe brain processing. Current approaches primarily probe cell-based variables, such as cytosolic calcium or membrane potential, but not cell-to-cell signaling. Here we introduce CNiFERS, cell-based neurotransmitter fluorescent engineered reporters, to address this challenge and monitor *in situ* neurotransmitter receptor activation. CNiFERS are cultured cells that are engineered to express a chosen metabotropic receptor, make use of the G_q protein-coupled receptor cascade to transform receptor activity into a rise in cytosolic [Ca²⁺], and report [Ca²⁺] with a genetically encoded fluorescent Ca²⁺ sensor. The initial realization of CNiFERS detects acetylcholine release via activation of M1 muscarinic receptors. Chronic implantation of M1-CNiFERS in frontal cortex of the adult rat is used to elucidate the muscarinic action of the atypical neuroleptics clozapine and olanzapine. We show that these drugs potently inhibit *in situ* muscarinic receptor activity.

A central tenet of neuronal processing is that unidirectional cell-to-cell communication is based on the release and subsequent binding of cell signaling molecules. Signaling can be localized to a pair of cells, as occurs with transmission across a synaptic cleft. Signaling can also occur within a volume of tissue through the diffusion of molecules away from the

Users may view, print, copy, download and text and data- mine the content in such documents, for the purposes of academic research, subject always to the full Conditions of use: http://www.nature.com/authors/editorial_policies/license.html#terms

Correspondence: Prof. David Kleinfeld University of California 9500 Gilman Drive La Jolla, CA 92093-0374 Phone - 858-822-0342 dk@physics.ucsd.edu.

Author Contributions

D.K., Q.-T.N. and L.F.S. designed and realized the CNiFERS, O.G. and M.M. synthesized the calcium indicator and consulted on molecular biology, D.K., A.M., Q.-T.N., L.F.S. and P.T. characterized and applied the CNiFERS, and D.K., Q.-T.N. and L.F.S. analyzed the data and wrote the manuscript.

cleft^{1, 2}. The spillover of glutamate, the excitatory transmitter among central synapses, leads to glutamatergic activation of extrasynaptic metabotropic receptors on nearby neurons and glia. Central modulators, including acetylcholine, serotonin, norepinephrine, and numerous neuropeptides, are commonly released directly into the extracellular space and have long-lasting and long-range effects on central processing. The dual nature of signaling, synaptic versus volume, suggests the possibility of different design strategies for functional probes of these two forms of communications.

The molecular detection of neuronal signaling molecules has achieved success for the case of glutamate through the fusion of pairs of fluorescent proteins with bacterial periplasmic proteins that bind small molecules³⁻⁵. Binding of glutamate leads to a structural change in the protein and a subsequent change in fluorescence resonance energy transfer (FRET) between the fluorescent proteins. Conceptually similar work involved the fusion of specific G-protein receptors with pairs of fluorescent proteins⁶. Such functionalized proteins are suitable for the detection of both synaptic and volume transmission. However, each molecular detector must be engineered *de novo* and used in combination with a suitable expression vector. We sought an alternate, modular approach for the detection of neuronal signaling molecules, with a focus on volume signaling.

Results

Our design exploits the modularity of G-protein receptors and their downstream pathways to expand on concepts from three past technological developments. First, cultured *Xenopus* myocytes that expressed nicotinic acetylcholine receptors have been used as *in vitro* electrophysiological reporters of pulsatile acetylcholine (ACh) release⁷. This work inspired the development of a cancerous cell line that expressed purinergic receptors for use as a detector of adenosine triphosphate release⁸. Second, high-throughput drug screening technologies can image receptor-transfected cells which are loaded with functional fluorescent dyes⁹. Third, implanted cultured cells filled with organic calcium indicators have been used as a test bed for fiber-optic imaging in rat cortex¹⁰. We express G-protein coupled receptors, whose inventory includes affinity for virtually every known signaling molecule, together with genetically expressible indicators of second messengers to create implantable cellular sensors of receptor activity.

This first realization of CNiFERs addresses the detection of acetylcholine (ACh) released into the extracellular space¹¹. This central modulator plays a prominent role in attention, learning and cortical plasticity¹² and is thought to influence the etiology of schizophrenia¹³. M1-CNiFERs are engineered from HEK293 cells that stably express the M1 receptor, a major muscarinic receptor in neocortex¹⁴, and the fusion-protein and calcium indicator TN-XXL¹⁵ (**Fig. 1a**). Activation of the M1 receptor increases cytosolic calcium in M1-CNiFERs via the G_q/IP₃ second messenger pathway. The subsequent binding of Ca²⁺ to TN-XXL induces a conformational change that enhances FRET between its cyan and yellow fluorescent protein domains¹⁵. Thus M1-CNiFERs report M1 receptor activity by a concurrent decrease in cyan and increase in yellow fluorescence. Lastly, control-CNiFERs express TN-XXL but not the M1 receptor; they are distinguished by expression of mCherry fluorescent protein (**Fig. 1a**).

The FRET response of M1-CNiFERS is studied under two-photon laser scanning microscopy¹⁶ (TPLSM); we report the change in FRET as

$$\frac{\Delta R(t)}{R} \equiv \frac{F_{\text{yellow}}(t)}{\langle F_{\text{yellow}}^{\text{baseline}} \rangle_{\text{prestim}}} / \frac{F_{\text{cyan}}(t)}{\langle F_{\text{cyan}}^{\text{baseline}} \rangle_{\text{prestim}}} - 1$$

where background values are subtracted from the individual fluorescent channels and the prestimulus period is typically 10 s. Bath application of an 500 s bolus of acetylcholine (1 to 1000 nM) reveals two time-scales of the M1-CNiFER response. An initial phasic response, with an EC₁₀ of 3 nM and an EC₅₀ of 11 nM, is followed by a plateau response with an EC₁₀ of 5 nM and an EC₅₀ of 9 nM (**Fig. 1b,c**). These values compare well with the 1 to 100 nM acetylcholine levels measured in rat brain with microdialysis^{17, 18}. Lastly, the phasic response is independent of external calcium concentration while the tonic response is abolished in calcium-free media (**Sup. Fig. 1**).

The phasic response was further probed with a fast perfusion system using 2.5 s applications of 60 or 100 nM acetylcholine, for which the peak responses are $F/F = 0.3$ and 0.9 , respectively (**Fig. 1d**). M1-CNiFERS respond within 2 s with a half-maximal rise-time of ~ 2 s, a full width at half maximal amplitude of ~ 7 s and can resolve pulses of 100 nM acetylcholine with an interstimulus interval as short as 6 s (**Fig. 1e**). Adaptation of the second response can be seen for the interstimulus interval of 21 s (**Fig. 1e**); further investigation reveals that the peak M1-CNiFER FRET response to pulses of acetylcholine adapts with a time constant of roughly 10^2 s towards an asymptotic value (**Sup. Fig. 2**). Lastly, we tested if M1-CNiFERS respond to a slowly increasing ramp in [ACh] that, in principle, could be undetected if adaptation is strong. For a concentration close to EC₅₀ reached over 10^3 s, sensitivity was maintained (**Sup. Fig. 3**).

The specificity of M1-CNiFERS was a concern since HEK293 cells can express endogenous surface receptors. We thus screened for potentially confounding receptor activation on a high-throughput fluorometric plate reader; the atropine sensitive response of M1-CNIFERS to a saturating level of acetylcholine ([ACh] = 100 nM) served as a reference (**Sup. Fig. 4**)

and we report $\delta R_{\text{M1}}^{\text{ligand}} \equiv \Delta R/R_{\text{M1}}^{\text{ligand}} / \Delta R/R_{\text{M1}}^{100 \text{ nM ACh}}$ and $\delta R_{\text{control}}^{\text{ligand}} \equiv \Delta R/R_{\text{control}}^{\text{ligand}} / \Delta R/R_{\text{M1}}^{100 \text{ nM ACh}}$. First, the activation of control-CNiFERS by acetylcholine is negligible, *i.e.*, $\delta R_{\text{control}}^{100 \text{ nM ACh}} < 0.05$ (**Fig. 1f,g**). Potentially confounding neurotransmitters typically have EC₅₀ > 1–10 μM and $\delta R_{\text{M1}}^{100 \text{ nM Ligand}} < 0.05$ (**Fig. 1g**).

Notable exceptions include norepinephrine ($\delta R_{\text{M1}}^{100 \text{ nM NE}} = 0.21$), adenosine ($\delta R_{\text{M1}}^{100 \text{ nM Ad}} = 0.19$), and vasoactive intestinal peptide ($\delta R_{\text{M1}}^{100 \text{ nM VIP}} = 0.33$) (**Fig. 1f,g**).

M1- and control-CNiFERS are implanted in discrete sites in frontal cortex of rat and imaged by TPLSM down to 300 μm below the cortical surface (**Fig. 2**). The typical imaging plane contains contributions from 10 to 30 CNiFERS per site. We test if implanted M1-CNiFERS are still functional by puffing acetylcholine from a pipette inserted near the implantation site. Volume injection of 5 to 50 nl of 1 mM acetylcholine, but not vehicle, elicit large

FRET responses in M1-CNIFERs (**Sup. Fig. 5**). To test that short, physiologically relevant bursts of endogenous acetylcholine will diffuse into the CNIFER sites at detectable concentrations, we electrically stimulate nucleus basalis magnocellularis (NBM), a basal forebrain structure that projects cholinergic fibers into neocortex. Single-train excitation of NBM induces a transient shift in the spectral content of the electrocorticogram that lowers the amplitude of the 1 to 6 Hz δ -band rhythms for several seconds (**Fig. 2b**); this pattern is a hallmark of NBM stimulation^{19, 20}. Concomitantly, M1-CNIFERs respond with a single peak initiated within 2 s, a half-maximal rise time of ~ 1 s and a width of less than 10 s; simultaneously imaged control-CNIFERs do not respond (**Fig. 2b**). This temporal resolution is comparable to that of electrochemistry and ~ 100 times faster than microdialysis. Lastly, we observe a strong correlation between electrocorticogram activation, measured as the Z-score of minus the logarithm of the power in the δ -band of the ECoG for a given animal, and response amplitude in M1, but not control, CNIFERs ($n = 4$ animals, 55 trials) (**Fig. 2c**), an anticipated result⁹.

The cholinergic nature of the *in vivo* M1-CNIFER response is verified by subcutaneous injection of physostigmine, an acetylcholinesterase inhibitor, that enhances the amplitude and duration of the NBM-evoked M1-CNIFER response for ~ 5000 s after injection ($n = 3$) (**Fig. 2d**). The ability of M1-CNIFERs to detect slow fluctuations in endogenous acetylcholine in the absence of NBM stimulation was tested by administering a relatively high dose of physostigmine to enhance the basal concentration of acetylcholine. We observe a concomitant enhancement in the M1- but not control-CNIFER FRET ($n = 3$) (**Fig. 2e**) that is accompanied by a reduction of power in the δ -band of the ECoG. Collectively, these acute experiments (**Fig. 2**) support the use of CNIFERs to detect small changes in the physiological release of acetylcholine.

Chronically implanted M1-CNIFERs can be imaged for at least six days (**Fig. 3a**). Imaging in the X-Z plane shows that the M1-CNIFER response to NBM stimulation extends throughout the depth of the implantation (**Fig. 3a**). The time dependence of the response is very similar to that found with acutely implanted M1-CNIFERs and, further, control-CNIFERs remain non-responsive (11 of 12 rats) (**Fig. 3b**). Images of intravenous fluorescein reveal patent vasculature around the implantations (**Sup. Fig. 6**) and immunohistochemistry demonstrates minimal tissue damage, negligible presence of reactive astrocytes, and no evidence for intracortical cell proliferation (**Sup. Fig. 7**). As confirmation that M1-CNIFERs respond to muscarinic activation, we observe that reverse dialysis of 1 to 5 μM atropine near the site of implantation acts to reduce the NBM-evoked M1-CNIFER response in a reversible manner ($n = 3$) (**Fig. 3c**); a dose of 100 μM atropine essentially abolishes the response ($n = 3$) (**Fig. 3c**). Pairs of NBM stimuli are resolvable by M1-CNIFERs with an interstimulus interval greater than 5 s (**Fig. 3d**), consistent with *in vitro* experiments (**Fig. 1e**). Finally, the response from chronically recorded M1-CNIFERs is monotonic with increasing stimulation intensity and duration (**Fig. 3e,f**), consistent with increased NBM recruitment and augmentation of acetylcholine release within cortex.

As a test bed for M1-CNIFERs, we address the action of a class of antipsychotic drugs, called atypical neuroleptics²¹, on cholinergic transmission. Atypical neuroleptics, the overwhelming preference for managing schizophrenia²², are primarily anti-dopaminergic

compounds with a broad spectrum of activity at other receptors. Many atypicals have marked cholinergic effects that are believed to contribute to their improved therapeutic properties²³. The atypicals olanzapine and clozapine elicit substantial acetylcholine release peripherally²⁴ and centrally^{25, 26}, though they are also muscarinic (**Sup. Fig. 4**)^{27, 28} and nicotinic antagonists²⁴. Furthermore, a bioactive metabolite of clozapine, n-desmethylclozapine, acts as a muscarinic receptor agonist²⁹. The net effect of atypicals on muscarinic transmission is debated³⁰. On the one hand, enhanced cholinergic release might explain the effectiveness of atypicals in improving cognition in schizophrenics^{29, 31}. On the other hand, antagonism of the muscarinic receptor can account for their favorable profile of extrapyramidal side effects²³. We use M1-CNIFERs to resolve these mutually exclusive alternatives.

We find that the atypical neuroleptic olanzapine profoundly depresses the M1-CNIFER FRET response to periodic stimulation of NBM. In contrast, essentially no change in the FRET response is seen after the injection of vehicle (**Fig. 4a**). The M1-CNIFER response in the presence of olanzapine is partially recovered by an increase in the amplitude of the NBM stimulation (**Fig. 4a**, red lines), suggestive of competitive inhibition. The suppressive effects of olanzapine on M1 receptor activation, as well as that of a second atypical neuroleptic, clozapine, is seen across a cohort of animals (n = 4 each) (**Fig. 4b,c**). Clozapine also suppresses NBM-evoked electrocorticogram activation, consistent with a blocking effect on endogenous M1 receptors *in vivo* (**Sup. Fig. 8**, olanzapine not tested). Further, suppression of M1-CNIFER activation by olanzapine is not dependent on repetitive stimulation, as olanzapine depresses the NBM-evoked response when NBM is first stimulated 1000 s after the injection of olanzapine (**Sup. Fig. 9**). As a final control, we find that the conventional antipsychotics chlorpromazine and haloperidol have no observable effect on the NBM-evoked M1-CNIFER response (n = 3 - 4 each) (**Fig. 4d,e**).

To test for olanzapine's net effect on extrasynaptic muscarinic transmission, as modeled by the response of chronically implanted M1-CNIFERs, we injected olanzapine at a dose known to increase cortical acetylcholine levels 6-fold²⁶. We find a negligible and statistically insignificant M1- as well as control-CNIFER FRET response (**Fig. 4f,g**). In contrast, nicotine ditartrate, which raises cortical acetylcholine levels 3-fold³², leads to a significant increase in the response of M1- but not control-CNIFERs (**Fig. 4f,g**). Collectively, the results with M1-CNIFERs indicate the atypical neuroleptics clozapine and olanzapine, unlike conventional antipsychotics, are potent *in vivo* inhibitors of extrasynaptic M1 muscarinic receptors as expressed in M1-CNIFERs implanted in frontal cortex. This occurs in spite of their marked ability to stimulate central acetylcholine release^{25, 26}. Our findings account for the reduced extrapyramidal side effects associated with atypical antipsychotic drugs, as these side effects and antimuscarinic activity are inversely related³³. They do not support the contention that clozapine and olanzapine activate extrasynaptic cortical M1 receptors indirectly via acetylcholine release.

Discussion

The response of CNIFERs will adapt upon exposure to a constant concentration of agonist. This appears as a phasic response that decays to a persistent, tonic level over $\sim 10^2$ s (**Figs.**

1b,c, and 4a). The phasic component does not depend on the external $[Ca^{2+}]$ (**Sup. Fig. 1**) and is consistent with a Ca^{2+} flux that derives from the endoplasmic reticulum as part of inositol triphosphate (IP_3) receptor-activation in the Gq-protein cascade³⁴. The transition from the larger amplitude of the phasic response to the smaller tonic response can result from a decrement in signaling molecule binding at any point in the muscarinic Gq-protein cascade. Past work implies that there is little desensitization or internalization of the M1 receptor³⁵. In contrast, $[Ca^{2+}]$ mirrors $[IP_3]$ and IP_3 exhibits both phasic and tonic components³⁶, similar to the components seen with CNiFERS (**Fig. 1b**). Thus a rate-limiting step in the generation of IP_3 , such as the availability of the intermediate phosphatidylinositol 4,5-bisphosphate³⁷, may explain the adaptation of the CNiFERS. A complementary explanation for the adaptation is that the tonic response is maintained via calcium flux through the cytoplasmic membrane rather than internal calcium stores, as evidenced by the abolishment of the tonic signal in calcium free media (**Sup. Fig. 1**).

CNiFERS indirectly report neurotransmitter release but directly report receptor sub-type activity, a measurement not possible using microdialysis, electrochemistry, or radioisotope tracers. They provide a general approach to observe the activation of G protein-coupled receptors by small molecules and peptides within living animals. CNiFERS for G_q protein-coupled receptors, such as those for the molecular transmitters serotonin and prostaglandins, can be engineered as an immediate extension of the M1-CNiFERS and their Ca^{2+} -based response. In contrast, CNiFERS for G_s and G_{i/o} protein-coupled receptors, such as those for the peptide transmitters vasoactive intestinal peptide and somatostatin, respectively, can be based on changes in the concentration of cAMP detected via a genetically encoded indicator for the activation of protein kinase A³⁸. Alternatively, an endogenous indicator for Ca^{2+} can be used if co-expressed with the promiscuous G_{α16}³⁹ or G_α chimeras⁴⁰; these G proteins allow receptors not normally linked with the G_q pathway to elicit cytosolic Ca^{2+} . Thus future CNiFERS may be realized to detect any signaling molecule, of which neurotransmitters are a broad and important class, that activates a G protein-coupled receptor.

Methods

Stably expressing cell lines

CNiFERS were created through replication deficient lentiviral transduction of HEK293 cells with cDNAs of the TN-XXL calcium indicator¹⁵, human M1 muscarinic receptor (gift from Paul Slesinger, Salk Institute), and mCherry fluorescent protein⁴¹ (gift from Roger Y. Tsien, UCSD). M1- and control-CNiFERS both express TN-XXL but are differentiated by either M1 receptor or mCherry expression, respectively. cDNAs were subcloned into HIV-based backbone cloning plasmids (System Biosciences, Mountain View, CA). Lentiviral particles were produced by the UCSD Vector Development Laboratory. Serial dilution clonal selection was assisted by puromycin (M1) and fluorescence (TN-XXL and mCherry). CNiFER clones were selected based on response to acetylcholine and fluorescence intensities. Clones were divided into aliquots and frozen with 10 % dimethyl sulfoxide at T = -80°C. CNiFERS were maintained at 37°C and 10 % CO₂ using Fisher Scientific 10 and Forma Scientific 3546 incubators (Thermo Scientific, MA). Upon confluence

(approximately twice weekly), cells were trypsinized, triturated, and seeded into new, 500 ml flasks with 0.2 μm filtered caps, using Dulbecco's Modification of Eagle's Medium (Cellgro®; Mediatech, Inc, VA) with addition of Glutamax™-1 (Invitrogen, CA) and 10 % (v/v) of Fetalplex™ serum (Gemini Bio-Products, CA). New aliquots of CNiFERs were thawed every 30 to 50 passages.

TPLSM imaging

CNiFERs were imaged with a custom two-photon laser scanning fluorescence microscope⁴² that runs the MPScope software suite⁴³. A femtosecond laser (Verdi oscillator with Mira pump laser, Coherent, Mountain View, CA) provided excitation light either at 760 nm to visualize mCherry, taking advantage of the anomalous excitation of mCherry at $\lambda < 780$ nm⁴⁴, or at 800 nm to excite the eCFP portion of TN-XXL while largely avoiding Citrine cp174. Fluorescence signals, collected either by 20X or 40X water dipping objectives (UIS2, Olympus, Center Valley, PA), were split into three channels: 455 to 495 nm (eCFP), 515 to 545 nm (eCFP and Citrine) and > 580 nm (mCherry). XY-image sizes were 256 by 256 or 512 by 512 pixels taken at 2 to 3 frames per second. XZ-imaging was achieved in line scan mode by moving the focal plane with a MIPOS 100 piezoelectric z-axis lens positioner (Piezosystem Jena, Jena, Germany) synchronized with the line scan. XZ-frames sizes were 256 by 256 pixels taken at 2 frames per second.

In vitro TPLSM testing

M1- and control-CNiFERs were plated on fibronectin-coated coverslips, placed in a cell culture chamber (RC26; Warner Instruments, CT) and perfused with artificial cerebral spinal fluid (ACSF: 125 mM NaCl, 5 mM KCl, 10 mM D-glucose, 10 mM HEPES, 3.1 mM CaCl_2 , 1.3 mM MgCl_2 , pH 7.4). Chamber fluid temperature was kept at 32°C by a temperature controller (TC-324B; Warner Instruments, CT). Rapid acetylcholine presentation was achieved with an actuated perfusion stepper (SF-77B; Warner Instruments, CT). The acetylcholine pipette was occasionally co-loaded with Alexa-594 to determine actual perfusion times. Bath acetylcholine presentation was delivered via gravity-feed.

In vitro high-throughput testing

FRET responses of M1- and control-CNiFERs to various ligands were measured *in vitro* using a high-throughput fluorometric plate reader (FlexStation® 3, Molecular Devices, Sunnyvale, CA). The day before experiments, M1- or control-CNiFERs were seeded in poly-D-lysine coated 96-well plates at 0.12×10^6 cells per well. Media was replaced in each well with 100 μl ACSF and plates were loaded into the FlexStation® 3. Experiments were conducted at 37°C using 435 nm excitation. Emitted light was collected at 485 nm and 527 nm every 3.8 s and ligand was delivered in 50 μl boluses without trituration. Background signals measured from neighboring wells without cells were subtracted, fluorescence intensities were normalized to pre-stimulus baselines, and peak responses selected from the ratio of the 527 nm and 485 nm channels. All peaks were then normalized by the M1-CNiFER response to maximal acetylcholine.

In vivo surgery and electrode placement

Adult male Sprague-Dawley rats (250-600 gm) were anesthetized with isoflurane according to standard protocol⁴⁵ and implanted with epidural 125 μm Teflon-coated silver-chloride wires across the imaging site for differential electrocorticogram (ECoG) recordings (A-M Systems Inc., WA). In each nucleus basalis magnocellularis (NBM) stimulation experiment, two 0.1 M Ω tungsten stimulating electrodes (Microprobes Inc., MD) spaced ~ 0.5 mm apart were implanted at the coordinates (2.1 mm, -1.2 mm, -6.9 mm)²⁰. Electrical stimulation consisted of 200 μs current-pulses of 100 to 1000 μA , at 100 Hz, for a duration of 20 to 500 ms. The depth of implantation and magnitude of current was adjusted to a value that would produce cortical activation, as assayed by reductions in cortical large-amplitude electrical oscillations⁴⁶; this value was typically 200 μA .

In vivo implantation

CNiFERs were trituated from culture flasks without trypsin, concentrated, and resuspended in ACSF for injection. After a craniotomy over frontal or parietal cortex and dural resection, CNiFERs were loaded into a ~ 40 μm inner-diameter glass pipette connected to a syringe pump and stereotaxically injected ~ 500 μm from the cortical surface using a syringe pump. Flow was stopped immediately after cells were seen to move down the pipette shaft, and pipette removal delayed for 5 min to prevent backflow of cells. In an attempt to avoid damage to the parenchyma this is far less than previous injection of transformed fibroblasts in *ex vivo* gene therapy experiments, which approximated 105 cells in 3 μl of media⁴⁷. After implantation in several adjacent sites, usually 4 to 5 sites for M1-CNiFERs and 2 to 3 for control-CNiFERs, the craniotomy was filled with 1.5 % agarose in ACSF and sealed with a coverslip using dental cement⁴⁸. Acute and chronic implantations were similar, except that in the latter, rats were immune-suppressed by daily cyclosporine injection (Belford Laboratories; 20 $\mu\text{l}/100$ gm, i.p.) starting one day before implantation. For acetylcholine puffing experiments an opening into the craniotomy was preserved to allow pipette insertion.

In vivo imaging

All *in vivo* imaging was performed under urethane (1.3-1.5 g/kg i.p.). For acetylcholine puffing, capillary pipettes with ~ 25 μm inner diameter were filled with PBS or 1 mM acetylcholine chloride in PBS and affixed to an oocyte injector (Nanoject II, Drummond, PA). The capillary tip was maneuvered into the window using a micromanipulator (MP-285; Sutter, CA) and positioned near the CNiFER implants. Experimental runs consisted of 10 s baselines followed by 5 to 50 nl injections. For NBM electrical stimulation experiments, 200 μs pulses of 100-1000 μA , at 20 Hz or 100 Hz, were delivered for a duration of 5 s or 20 to 500 ms, respectively. Electrocorticogram signals were amplified with a DAM80 differential amplifier (World Precision Instruments, CT), using a bandpass of 0.1 to 100 Hz, and gain of 1000. Cerebrovasculature was visualized by injecting 500 μl of 5 % (w/v) fluorescein dextran (Sigma; I.V.).

***In vivo* pharmacology**

For acetylcholinesterase inhibition experiments, subcutaneous physostigmine salicylate in 100 mM phosphate-buffered saline was injected at 200 or 300 µg/kg. Intracerebral atropine perfusion was performed by a syringe pump connected to a microdialysis probe (CMA 11; CMA, North Chelmsford, MA) implanted 1000 µm into cortex and ~2 mm from CNiFERs. Flow rate was set to 2 to 15 µl/min. Neuroleptics were dissolved in vehicle using 1 % (v/v) glacial acetic acid in PBS and a total volume of 1 ml/kg was injected intraperitoneally. Atypical neuroleptics were used at dosages similar to those in other studies designed to match human therapeutic plasma drug levels^{30, 49}. Nicotine ditartrate was used for nicotine experiments and delivered in a volume of 1 ml/kg intraperitoneally. Drugs were purchased from Sigma or A.G. Scientific.

Data analysis

All TN-XXL fluorescence intensities were background-subtracted and normalized to pre-stimulus baselines, as noted in the equation in the text, as R/R . *In vitro*, images were averaged to include all cells in the field of view. *In vivo*, regions of interest were drawn around either M1- or control-CNiFER implants generally encompassing 10 to 150 cells.

For ECoG time-series epochs, spectral power densities were estimated using the multi-taper algorithm in Chronux Analysis Software for Matlab (<http://chronux.org>). Post-stimulus time-series consisted of a single 5 s epoch beginning 600 ms after NBM stimulus onset. Baseline epochs consisted of four, 5 s epochs immediately preceding NBM stimulus onset. We chose a time-bandwidth product of 5 for 9 tapers. The measure of δ -band ECoG activity was found by: (1) calculating the spectral power of each time series, where the time series for the n -th trial is denoted $V_n(t)$ and the corresponding spectral power is denoted $\tilde{S}_n(f)$; (2) calculating the power in the 1 to 6 Hz δ -band as $\tilde{S}_n^{(\delta)} = \int_{1\text{ Hz}}^{6\text{ Hz}} \tilde{S}_n(f) df$; (3) taking the logarithm of $\tilde{S}_n^{(\delta)}$, which is χ^2 -distributed, to form the Gaussian distributed variable $\tilde{P}_n^{(\delta)} \equiv -\log_e \tilde{S}_n^{(\delta)}$; where the minus sign reflects the decrease in power with increasing activation; (4) Z-score equalizing the log-power as

$$\left(\tilde{P}_n^{(\delta)} - \langle \tilde{P}^{(\delta)} \rangle \right) / \sqrt{\left\langle \left(\tilde{P}_n^{(\delta)} - \langle \tilde{P}^{(\delta)} \rangle \right)^2 \right\rangle}$$

to permit comparisons between animals.

Smoothed lines for CNiFER responses made with the Bayesian adaptive regression splines nonparametric smoothing algorithm for normally distributed data (**Figs. 1b and 2d,e**)⁵⁰ (<http://www.stat.cmu.edu/~jliebner/>).

Histological Procedure Adult animals were perfused with phosphate buffered saline (PBS) for the generation of fresh tissue. The typical perfusion volumes were 0.5 ml per gram animal and flow rates were 20 ml/min. The PBS perfusion was immediately followed by a second perfusion with 4 % (w/v) paraformaldehyde (PFA) in PBS. The extracted brain was stored in 4 % PFA in PBS for post-fixation. Blocking of the tissue, if necessary, was done with a mounted razor blade. α -GFAP rabbit antibodies (Zymed, CA) were used to visualize astrocytes. Sections were quenched in 3% hydrogen peroxide for 15 minutes then incubated overnight in a 1:200 dilution of primary α -GFAP antibody in the diluent used throughout the

histological process: PBS containing 0.25% Triton, 5% goat serum and 0.02% sodium azide. After washing for 1 hour, α -GFAP sections were incubated in a 1:500 dilution of biotinylated α -rabbit secondary antibody (Vector Laboratories, CA). This was followed by the avidin:biotinylated complex method (Vectastain ABC kit, Vector Laboratories, CA) and 3,3'-diaminobenzidine (DAB) visualization with nickel. Sections were mounted on slides and imaged on an upright microscope with brightfield for DAB stains and epifluorescence for M1- and control-CNiFERs.

Supplementary Material

Refer to Web version on PubMed Central for supplementary material.

Acknowledgements

We are grateful to T. Bartfai, D. K. Berg, J.-P. Changeux, J. M. Edeline, A. L. Fairhall, B. Hille, H. J. Karten, R. Metherate, A. Muller, P. A. Slesinger, T. Talley, R. Y. Tsien and M. Tuzsinsky for valuable discussions. We thank R. Figueroa for maintaining the cell culture facility, J. Groisman for preparing the artwork in figure 3a, and A. Miyanojara (Vector Development Laboratory, Human Gene Therapy Program, UCSD) for producing the lentiviruses. Supported by the NIH Medical Scientist Training Program (L.F.S.), the Max Planck Society (O.G.), and grants from the NIH (DA024206, EB003832, and MH085499 to D.K., GM18360 and DA19372 to P.T., and MH070655 to Q.-T.N.).

Abbreviations

Ach	Acetylcholine
CNiFER	Cell-based neurotransmitter fluorescent engineered reporter
EC₁₀	Effective concentration for 10 % response level
EC₅₀	Effective concentration for 50 % response level
ECoG	Electrocorticogram
FRET	Fluorescence resonance energy transfer
IP₃	Inositol triphosphate
NBM	Nucleus basalis magnocellularis
TPLSM	Two-photon laser scanning microscopy

REFERENCES

1. Agnati LF, et al. Volume transmission and wiring transmission from cellular to molecular networks: History and perspectives. *Acta Physiology (Oxford)*. 2006; 1-2:529–344.
2. Beaudet A, Descarries L. The monoamine innervation of rat cerebral cortex: Synaptic and nonsynaptic axon terminals. *Neuroscience*. 1978; 3:851–860. [PubMed: 215936]
3. Tsien RY. Building and breeding molecules to spy on cells and tumors. *FEBS Letters*. 2005; 579:927–932. [PubMed: 15680976]
4. Hires SA, Zhu Y, Tsien RY. Optical measurement of synaptic glutamate spillover and reuptake by linker optimized glutamate-sensitive fluorescent reporters. *Proceeding of the National Academy of Sciences*. 2008; 105:4411–4416.
5. Okumoto S, et al. Detection of glutamate release from neurons by genetically encoded surface-displayed FRET nanosensors. *Proceedings of the National Academy of Sciences USA*. 2005; 102:8740–8745.

6. Vilardaga J-P, Bünemann M, Krasel C, Castro M, Lohse MJ. Measurement of the millisecond activation switch of G protein-coupled receptors in living cells. *Nature Biotechnology*. 2003; 12:807–812.
7. Young SH, Poo MM. Spontaneous release of transmitter from growth cones of embryonic neurones. *Nature*. 1983; 305:634–637. [PubMed: 6312327]
8. Haas B, et al. Activity-dependent ATP-waves in the mouse neocortex are independent from astrocytic calcium waves. *Cerebral Cortex*. 2005; 16:237–246. [PubMed: 15930372]
9. Schroeder KS, Neagle B. FLIPR: A new instrument for accurate, high throughput optical screening. *Journal of Biomolecular Screening*. 1995; 1:75–80.
10. Duff Davis M, Schmidt JJ. In vivo spectrometric calcium flux recordings of intrinsic Caudate-Putamen cells and transplanted IMR-32 neuroblastoma cells using miniature fiber optrodes in anesthetized and awake rats and monkeys. *Journal of Neuroscience Methods*. 2000; 99:9–23. [PubMed: 10936638]
11. Umbriaco D, Watkins KC, Descarries L, Cozzari C, Hartman BK. Ultrastructural and morphometric features of the acetylcholine innervation in adult rat parietal cortex: an electron microscopic study in serial sections. *Journal of Comparative Neurology*. 1994; 348:351–373. [PubMed: 7844253]
12. Everitt BJ, Robbins TW. Central cholinergic systems and cognition. *Annual Review of Psychology*. 1997; 48:649–684.
13. Raedler TJ, et al. Towards a muscarinic hypothesis of schizophrenia. *Molecular Psychiatry*. 2007; 12:232–246. [PubMed: 17146471]
14. Levey AI, Kitt CA, Simonds WF, Price DL, Brann MR. Identification and localization of muscarinic acetylcholine receptor proteins in brain with subtype-specific antibodies. *Journal of Neuroscience*. 1991:3218–3226. [PubMed: 1941081]
15. Mank M, et al. A genetically encoded calcium indicator for chronic in vivo two-photon imaging. *Nature Methods*. 2008; 5:805–811. [PubMed: 19160515]
16. Denk W, Strickler JH, Webb WW. Two-photon laser scanning fluorescence microscopy. *Science*. 1990; 248:73–76. [PubMed: 2321027]
17. Rasmusson DD, Clow K, Szerb JC. Frequency-dependent increase in cortical acetylcholine release evoked by stimulation of the nucleus basalis magnocellularis in the rat. *Brain Research*. 1992; 594:150–154. [PubMed: 1467935]
18. Day JC, Kornecook TJ, Quirion R. Application of in vivo microdialysis to the study of cholinergic systems. *Methods*. 2001; 23:21–39. [PubMed: 11162147]
19. Rasmusson DD, Clow K, Szerb JC. Modification of neocortical acetylcholine release and electroencephalogram desynchronization due to brainstem stimulation by drugs applied to the basal forebrain. *Neuroscience*. 1994; 60:665–677. [PubMed: 7936193]
20. Berg RW, Friedman B, Schroeder LF, Kleinfeld D. Activation of nucleus basalis facilitates cortical control of a brainstem motor program. *Journal of Neurophysiology*. 2005; 94:699–711. [PubMed: 15728764]
21. Meltzer HY. What's atypical about atypical antipsychotic drugs? *Current Opinions in Pharmacology*. 2004; 4:53–57.
22. Snyder EM, Murphy MR. Schizophrenia therapy: Beyond atypical antipsychotics. *Nature Reviews Drug Discovery*. 2008; 7:471–472.
23. Bymaster FP, et al. Muscarinic mechanisms of antipsychotic atypicality. *Progress in Neuropsychopharmacological and Biological Psychiatry*. 2003; 27:1125–1143.
24. Nguyen QT, Yang J, Miledi R. Effects of atypical antipsychotics on vertebrate neuromuscular transmission. *Neuropharmacology*. 2002; 42:670–676. [PubMed: 11985825]
25. Parada MA, Hernandez L. Selective action of acute systemic clozapine on acetylcholine release in the rat prefrontal cortex by reference to the nucleus accumbens and striatum. *Journal of Pharmacology and Experimental Therapeutics*. 1997; 281:582–588.
26. Ichikawa J, Dai J, O'Laughlin IA, Fowler WL, Meltzer HY. Atypical, but not typical, antipsychotic drugs increase cortical acetylcholine release without an effect in the nucleus accumbens or striatum. *Neuropsychopharmacology*. 2002; 26:325–339. [PubMed: 11850147]

27. Bolden C, Cusack B, Richelson E. Antagonism by antimuscarinic and neuroleptic compounds at the five cloned human muscarinic cholinergic receptors expressed in Chinese hamster ovary cells. *Journal of Pharmacology and Experimental Therapeutics*. 1992; 260:576–580. [PubMed: 1346637]
28. Chew ML, et al. A model of anticholinergic activity of atypical antipsychotic medications. *Schizophrenia Research*. 2006; 88:63–72. [PubMed: 16928430]
29. Davies MA, Compton-Toth BA, Hufeisen SJ, Meltzer HY&L, R.B. The highly efficacious actions of N-desmethylozapine at muscarinic receptors are unique and not a common property of either typical or atypical antipsychotic drugs: Is M1 agonism a prerequisite for mimicking clozapine's actions. *Psychopharmacology (Berlin)*. 2005; 178:451–460. [PubMed: 15765260]
30. Johnson DE, et al. The role of muscarinic receptor antagonism in antipsychotic-induced hippocampal acetylcholine release. *European Journal of Pharmacology*. 2005; 506:209–219. [PubMed: 15627430]
31. Gray JA, Roth BL. Molecular targets for treating cognitive dysfunction in schizophrenia. *Schizophrenia Bulletin*. 2007; 33:1100–1119.
32. Tani Y, Saito K, Imoto M, Ohno T. Pharmacological characterization of nicotinic receptor-mediated acetylcholine release in rat brain: An in vivo microdialysis study. *European Journal of Pharmacology*. 1998; 351:181–188. [PubMed: 9687001]
33. Snyder S, Greenberg D, Yamamura HI. Antischizophrenic drugs and brain cholinergic receptors. Affinity for muscarinic sites predicts extrapyramidal effects. *Archives of General Psychiatry*. 1974; 31:58–61. [PubMed: 4152054]
34. Krasel C, Vilardaga JP, Bunemann M, Lohse MJ. Kinetics of G-protein-coupled receptor signalling and desensitization. *Biochemical Society Transactions*. 2004; 32:1029–1031. [PubMed: 15506955]
35. Vogler O, et al. Receptor subtype-specific regulation of muscarinic acetylcholine receptor sequestration by dynamin. Distinct sequestration of m2 receptors. *Journal of Biological Chemistry*. 1998; 273:12155–12160.
36. Willars GB, Nahorski SR. Quantitative comparisons of muscarinic and bradykinin receptor-mediated Ins (1,4,5)P3 accumulation and Ca²⁺ signalling in human neuroblastoma cells. *British Journal of Pharmacology*. 1995; 114:1133–1142. [PubMed: 7620702]
37. Horowitz LF, et al. Phospholipase C in living cells: Activation, inhibition, Ca²⁺ requirement, and regulation of M current. *Journal of General Physiology*. 2005; 126:243–262. [PubMed: 16129772]
38. Zhang J, Hupfeld CJ, Taylor SS, Olefsky JM, Tsien RY. Insulin disrupts betaadrenergic signalling to protein kinase A in adipocytes. *Nature*. 2005; 437:569–573. [PubMed: 16177793]
39. Kostenis E, Waelbroeck M, Milligan G. Techniques: Promiscuous Galpha proteins in basic research and drug discovery. *Trends in Pharmacological Science*. 2005; 26:595–602.
40. Coward P, Chan SD, Wada HG, Humphries GM, Conklin BR. Chimeric G proteins allow a high-throughput signaling assay of Gi-coupled receptors. *Analytical Biochemistry*. 1999; 270:242–248. [PubMed: 10334841]
41. Shaner NC, et al. Improved monomeric red, orange and yellow fluorescent proteins derived from *Discosoma* sp. red fluorescent protein. *Nature Biotechnology*. 2004; 22:1567–1572.
42. Tsai, PS.; Kleinfeld, D. In vivo two-photon laser scanning microscopy with concurrent plasma-mediated ablation: Principles and hardware realization.. In: Frostig, RD., editor. *Methods for In Vivo Optical Imaging*. 2nd edition. CRC Press; Boca Raton: 2009. p. 59-115.
43. Nguyen, Q-T.; Dolnick, EM.; Driscoll, J.; Kleinfeld, D. MPScope 2.0: A computer system for two-photon laser scanning microscopy with concurrent plasma-mediated ablation and electrophysiology.. In: Frostig, RD., editor. *Methods for In Vivo Optical Imaging*. 2nd edition. CRC Press; Boca Raton: 2009. p. 117-142.
44. Drobizhev M, Tillo S, Makarov NS, Hughes TE, Rebane A. Absolute two-photon absorption spectra and two-photon brightness of orange and red fluorescent proteins. *Journal of Chemical Physics B*. 2009; 113
45. Schaffer CB, et al. Two-photon imaging of cortical surface microvessels reveals a robust redistribution in blood flow after vascular occlusion. *Public Library of Science Biology*. 2006; 4:258–270.

46. Metherate R, Ashe JH. Ionic flux contributions to neocortical slow waves and nucleus basalis-mediated activation: Whole-cell recordings in vivo. *Journal of Neuroscience*. 1993; 12:5312–5323. [PubMed: 8254377]
47. Kawaja MD, Gage FH. Morphological and neurochemical features of cultured primary skin fibroblasts of Fischer 344 rats following striatal implantation. *Journal of Comparative Neurology*. 1992; 317:102–116. [PubMed: 1573056]
48. Nishimura N, et al. Targeted insult to individual subsurface cortical blood vessels using ultrashort laser pulses: Three models of stroke. *Nature Methods*. 2006; 3:99–108. [PubMed: 16432519]
49. Shirazi-Southall S, Rodriguez DE, Nomikos GG. Effects of typical and atypical antipsychotics and receptor selective compounds on acetylcholine efflux in the hippocampus of the rat. *Neuropsychopharmacology*. 2002; 26:583–594. [PubMed: 11927183]
50. DiMatteo I, Genovese CR, Kass RE. Bayesian curve-fitting with free-knot splines. *Biometrika*. 2001; 88:1055–1071.

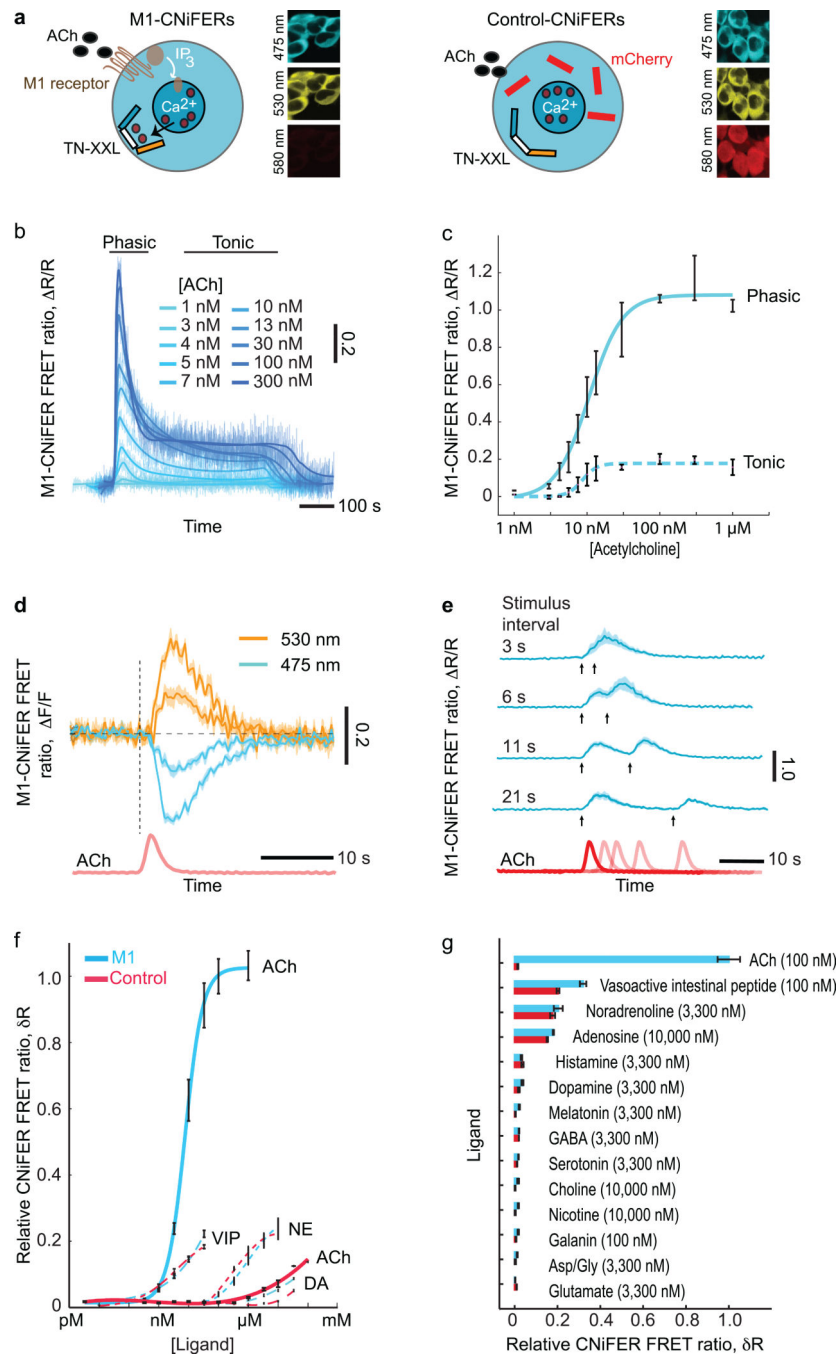


Figure 1. Design and *in vitro* characterization of CNiFERS

(a) CNiFERS used in this study are HEK293 cells that stably express the M1 muscarinic receptor and the FRET-based calcium indicator TN-XXL (M1-CNiFERS), or TN-XXL and mCherry (control-CNiFERS) (Methods in Supplemental Material). In M1-CNiFERS, acetylcholine is depicted as activating M1 to induce IP₃-mediated Ca²⁺ cytoplasmic influx detected by TN-XXL. Fluorescence from the eCFP (cyan) and Citrine cp174 (yellow) fluorescent proteins incorporated into TN-XXL are collected for the FRET-based signal. (b) M1-CNiFERS respond to an 500 s bath application of acetylcholine with two time-scales: a

phasic response that peaks within ~ 20-40 s and a tonic plateau that stabilizes after ~ 300 s. **(c)** M1-CNiFER phasic response to acetylcholine is monotonic in the range 1 – 100 nM, with an EC_{50} of 11 nM, a Hill coefficient of 1.9, and a maximum of $R/R = 1.1$. The tonic response is monotonic in the range 5-30 nM, with an EC_{50} of 9 nM, a Hill coefficient of 4.4 and a maximum of $R/R = 0.18$. Phasic responses are measured as the maximum value of R/R between 0 and 100 s after lowpass filtering of the data at 0.3 Hz, while tonic responses are measured as the average value of R/R between 300 and 400 s ($n = 3$). **(d)** Acetylcholine presentation of ~2.5 s (red trace) to M1-CNiFERs leads to opposing responses in cyan (475 nm) versus yellow (530 nm) fluorescence. The response initiates within 2 s with a full-width half maximal response of ~ 7 s ($n = 5$). **(e)** Two M1-CNiFER FRET-based responses to 100 nM acetylcholine can be discriminated with an interstimulus interval of 6 s or longer ($n = 3$). **(f)** Dose-response of M1-CNiFERs (cyan) and control-CNiFERs (red) to a subset of endogenous neurotransmitters: acetylcholine (ACh), vasoactive intestinal peptide (VIP), norepinephrine (NE), and dopamine (DA) ($n = 5$). **(g)** Summary of screening data at physiologically relevant concentrations reveals that M1-CNiFERs respond with greatest amplitude to acetylcholine, while control-CNiFERs are non-responsive to acetylcholine ($n = 3 - 5$). All bars are standard errors.

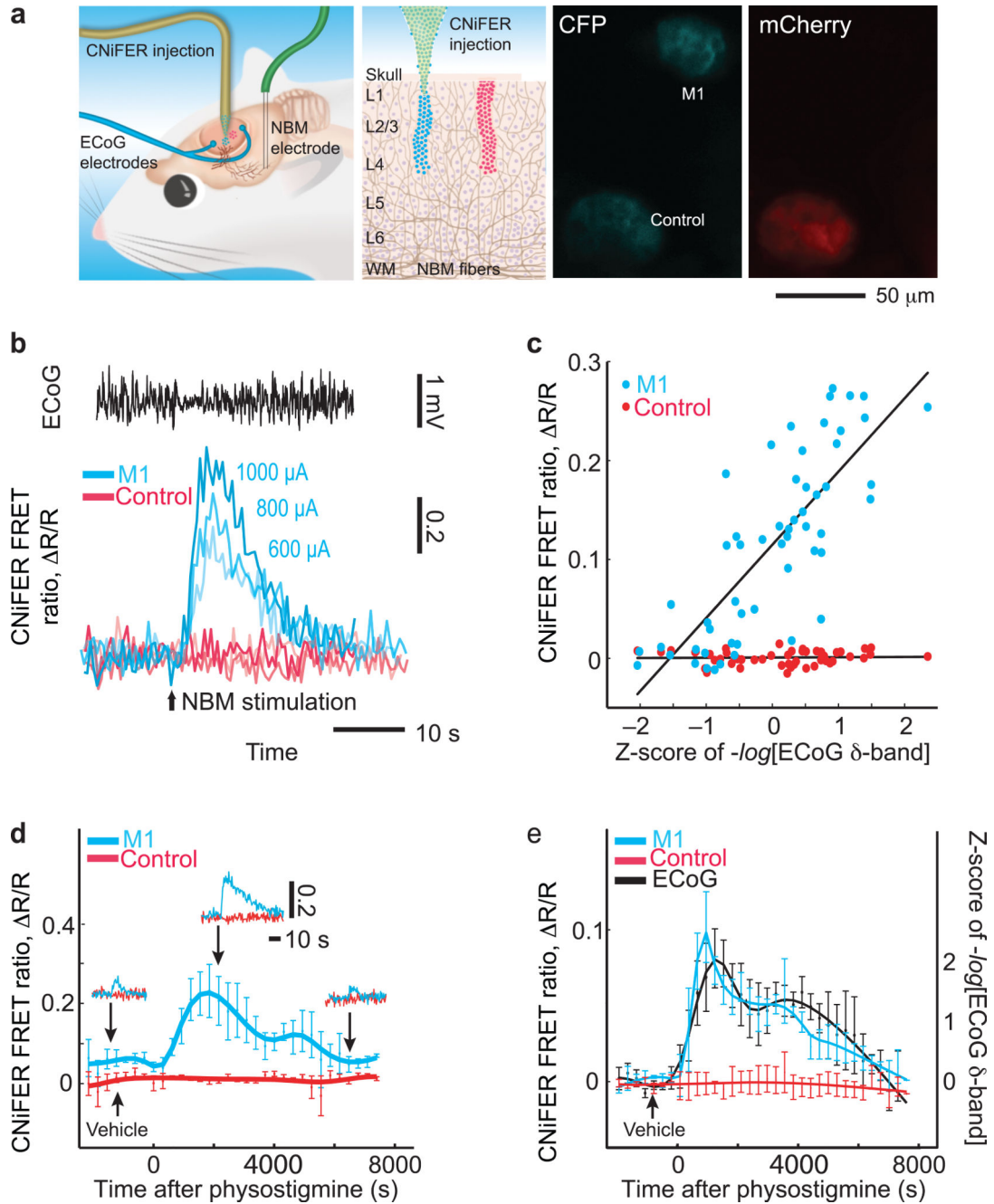


Figure 2. *In vivo* characterization of acutely implanted M1-CNIFERs

(a) Stimulating electrodes are implanted in NBM to recruit the cortical afferent cholinergic system, and electrocorticogram wires are placed to detect NBM-evoked cortical activation (Methods in Supplemental Material). M1-CNIFERs and control-CNIFERs are implanted in separate columns in neocortex, where cholinergic terminals are widely distributed, and imaged acutely or chronically using two-photon laser scanning microscopy. To the right, a two-photon microscopy image of M1-CNIFERs (cyan) and control-CNIFERs (red) implanted in rat motor cortex in 25 – 50 μm diameter columns. Data represent a Z-projection from 40 – 60 μm below the cortical surface. There are ~ 10 – 20 CNiFER cells per site in

this field of view. **(b)** M1-CNiFER FRET responses (lower) and ECoG activity (upper) evoked by increasing levels of NBM electrical stimulation. Cortical activation appears as a shift from large to small amplitude waves. Control-CNiFERs are non-responsive. **(c)** M1-CNiFER response to NBM stimulation is strongly correlated to loss of power in the electrocorticogram δ -band, quantified as the Z-score normalized logarithm of the reciprocal of the power, $-\log[\text{power in ECoG } \delta\text{-band}]$, for each animal (Methods; Supplemental Material). CNiFER responses are defined as the area under the curve of R/R for 10 s after the stimulus normalized to that of 10 s before the stimulus ($n = 55$ trials with 4 animals). **(d)** Subcutaneous physostigmine salicylate at 200 $\mu\text{g}/\text{kg}$ enhances the amplitude and duration of M1-CNiFER response to NBM stimulation. The response disappears by ~ 8000 s. Data in bottom trace represent the fractional change of $1/3$ the area under the curve of R/R for 30 seconds after the stimulus as compared to that of 10 s before the stimulus. Top traces are examples of raw data used to calculate bottom trace; NBM stimulation occurs every 300 s and vehicle in PBS ($n = 3$). **(e)** Subcutaneous physostigmine salicylate at 300 $\mu\text{g}/\text{kg}$ causes an increase in baseline M1-CNiFER FRET fluorescence over ~ 8000 s. This appears to result from modulation of background levels of acetylcholine in cortex. M1-CNiFERs (cyan) and control-CNiFERs (red) measured as an average over 10 s every 300 s (top). All measurements are normalized to first 3 measurements before vehicle injection, and not to internal baselines, thus preserving the tonic response. Data from 4 consecutive 300 s epochs for each animal ($n = 4$), and plotted in black at each time point (bottom). All bars are standard errors.

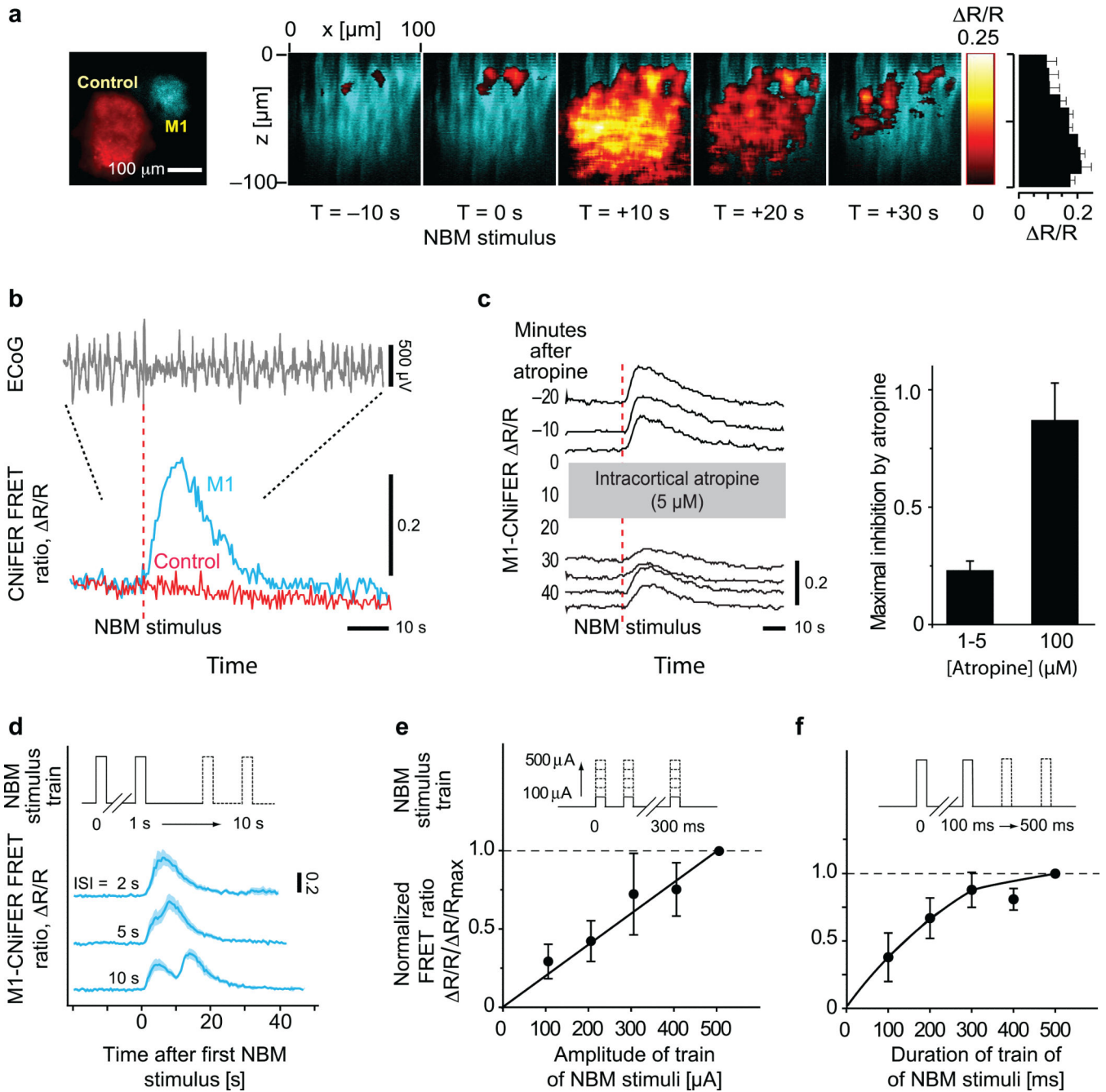


Figure 3. Chronic implantation of CNiFERS

(a) Chronically implanted M1- and control-CNiFER sites are shown on the left, a X-Z time series from the M1-CNiFERS in response to a single-train NBM stimulation is shown in the center and the average intensity (mean \pm standard error; n = 4 animals) of the M1-CNiFER response as a function of depth is shown on the right. (b) Electrocardiogram and FRET responses in M1- and control-CNiFERS in response to NBM stimulation; 300 ms train of 300 μA pulses (Methods; Supplemental Material). (c) Atropine antagonism. Left traces: M1-CNiFER responses to single-train NBM stimulation are inhibited by reverse dialysis of intracortical atropine sulfate. Bar graph: average peak inhibition of CNiFER response due to

1 – 5 μM atropine ($23 \pm 4 \%$) ($n = 4$ rats) or 100 μM atropine ($87 \pm 16 \%$) ($n = 3$ rats). **(d)** Temporal resolution of acutely implanted M1-CNiFERS. Top pane: stimulation protocol. Traces: Each trace represents the mean response of M1-CNiFERS to two consecutive stimulations of NBM ($n = 5$ for each condition, repeated over 3 animals). **(e)** Response of M1-CNiFERS versus stimulation current. Top pane: stimulation protocol. Graph: average M1-CNiFER response normalized to that at 500 μA ($n = 6$ rats). **(f)** Response versus duration of the stimulation train. Top pane: stimulation protocol. Graph: average M1-CNiFER response normalized to that at 500 ms ($n = 6$ rats). The black curves in (e) and (f) are visual aids.

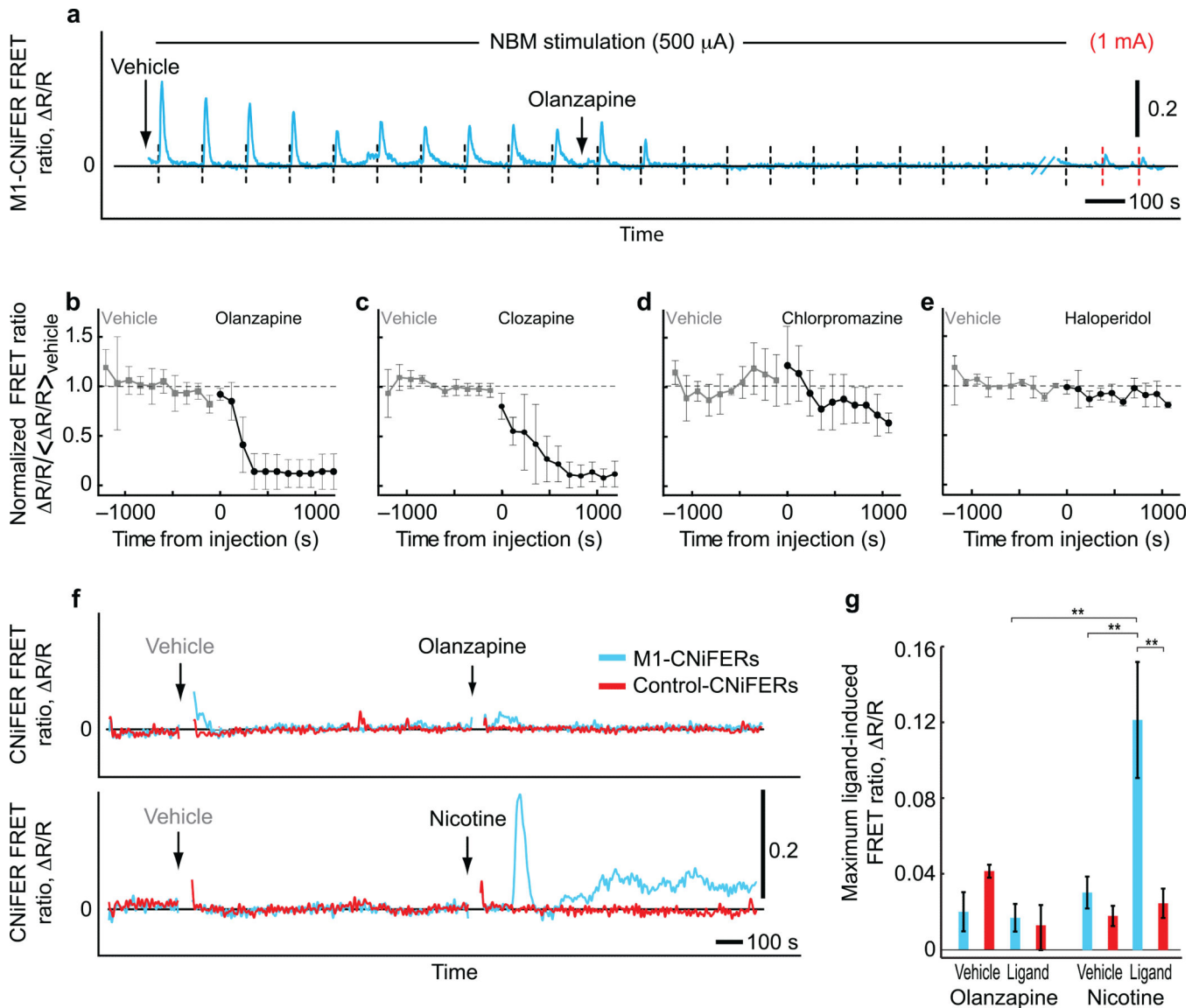


Figure 4. *In vivo* pharmacology of chronically implanted M1-CNiFERS

(a) Olanzapine intraperitoneal injection at 3 mg/kg suppresses the M1-CNiFER response elicited by repetitive NBM stimulation (500 μ A; black vertical dashed lines). The M1-CNiFER response is partially recovered by increasing the amplitude of NBM stimulation (1 mA; red vertical dashed lines). (b-e) Atypical, but not conventional, antipsychotics suppress the M1-CNiFER response elicited by NBM stimulation. Graphs: M1-CNiFER peak response normalized to those averaged during vehicle injection; olanzapine at 3-5 mg/kg (n = 4); clozapine at 5 mg/kg (n = 4); chlorpromazine at 5 mg/kg (n = 4); and haloperidol at 1 mg/kg (n = 3). Grey: vehicle. Black: antipsychotic. (f) Olanzapine, injected i.p. at a dose of 10 mg/ml, does not elicit a response in M1-CNiFERS while nicotine ditartrate (green), injected i.p. at a dose of 1 mg/ml elicits a response. (g) Composite results (n = 4 rats) of the maximum response, measured between 120 and 720 s after injection. The response of M1-

CNiFERS to nicotine is significantly greater than that for controls, while the response of M1-CNiFERS to olanzapine is at chance. **Significantly different values by t-test ($p < 0.05$).

Author Manuscript

Author Manuscript

Author Manuscript

Author Manuscript